FM 7245

Growth of Bioconvection Patterns in a Suspension of Gyrotactic Micro-organisms in a Layer of Finite Depth

by

N.A. Hill, T.J. Pedley

Department of Applied Mathematics and Theoretical Physics,
University of Cambridge, Silver Street, Cambridge CB3 9EW,
United Kingdom

and

J.O. Kessler, Department of Physics, University of Arizona
Tucson, AZ 85721, U.S.A.

Extended version of Section 4 to be held in the editorial files of the Journal of Fluid Mechanics.

4. Asymptotic analysis

A number of limiting cases are analysed asymptotically in this section. The results are summarised in Table 1 and Figure 1. The exponential term in equation (3.12) makes it appropriate to consider two limits for asymptotic analysis. In the shallow layer approximation $d << 1$, i.e. the layer depth H is much less than the length scale ℓ of the equilibrium density distribution, and the exponential term is approximately linear, with consequent simplification. For a deep layer, d is large and, in the basic state, the cells are concentrated in a boundary layer at the upper surface, so that the method of matched asymptotic expansions can be used.

The purpose of the subsequent asymptotic analysis is to give insight into the fluid mechanics of bioconvection and to provide checks on the numerical solutions of §5. Wherever possible σ is taken to be complex and non-zero, but in many cases the analysis becomes so complicated that it is necessary to resort to numerical solutions of transcendental equations, which offer little analytical insight. In such cases attention is confined to the neutral curves on which $\mathrm{Re}(\sigma) = 0$. Moreover, for all the parameter values considered analytically below, the numerical solution shows that $\mathrm{Im}(\sigma)$ vanishes, i.e. there are only stationary solutions. Attempts at asymptotic solutions for other parameter values lead to such complications that the numerical solutions of §5 are preferred; such parameter values do sometimes exhibit oscillatory instability.

4.1 Shallow layer approximation, $0 < d << 1$

Rather than solving (3.15) in the shallow layer approximation, it is more convenient to consider equations (3.11) and (3.12), which we rewrite as

$$(\frac{d^2}{dz^2} - d^2\tilde{k}^2 - \frac{\sigma}{S_c})(\frac{d^2}{dz^2} - d^2\tilde{k}^2)W = -dR\tilde{k}^2\Phi \ , \tag{4.1}$$

and

$$(\frac{d^2}{dz^2} - d\frac{d}{dz} - d^2\tilde{k}^2 - \sigma)\Phi = d(1 + dz + d^2z^2/2 + ...)\times$$
$$[1 - G(1+\alpha_0)d^2/dz^2 + d^2\tilde{k}^2G(1-\alpha_0)]W \ , \tag{4.2}$$

where

$$\tilde{k} = k/d \ . \tag{4.3}$$

The leading order versions of equations (4.1) and (4.2) can be solved in principle by elementary methods. However, once the boundary conditions are applied, the solution for the neutral curve $R(k; G, \alpha_0)$ leads to a transcendental equation, which has to be solved numerically. Instead, we choose to simplify (4.1) and (4.2) further to gain a better understanding of the analysis and to obtain results which can be compared with the numerical solution of the full linear stability problem in §5 below. Therefore we first consider small wavenumbers where $k \sim d$ and so

$$\tilde{k} \sim 1 \ . \tag{4.4}$$

This is equivalent to scaling k^* on ℓ^{-1} rather than H^{-1}, and corresponds to a horizontal planform of wavelength $\lambda^* \sim \ell$, much greater than the layer depth H.

We now concentrate on the analysis of neutral curves and examine the possible balances between the terms in (4.1) and (4.2) which indicate the relevant asymptotic expansions. For non-vanishing solutions, which satisfy the six, leading order, boundary conditions

$$\frac{d\Phi}{dz} = W = \frac{dW}{dz} = 0 \text{ at } z = -1, 0 \ , \tag{4.5}$$

the highest order derivatives in (4.1) and (4.2) must be retained at leading order. It is also readily shown that in each of the cases discussed below the leading order balance in (4.1) must give

$$(\frac{d^2}{dz^2} - \frac{\sigma}{S_c})\frac{d^2W}{dz^2} = -dR\tilde{k}^2\Phi \ , \tag{4.5}$$

otherwise there is only the trivial solution. Moreover (4.5) represents the balance between the viscous term d^4W/dz^4 and the buoyancy force on the right hand side which drives the flow. Without loss of generality, we also specify that

$$\Phi = O(1) \ . \tag{4.7}$$

There are then four possible, leading order balances between the terms in (4.2) which are shown below, together with the appropriate leading order versions of (4.2), which we recall is derived from the cell conservation equation (2.3), when $\sigma = 0$.

Case I:

$$G \leq O(d^{-1}), \ R \sim 1 \ .$$

$$d^2\Phi/dz^2 = 0 \ .$$

Case II:

$$G \leq O(d), \ R \sim d^{-2} \ .$$

$$d^2\Phi/dz^2 = dW \ .$$

Case III:

$$G \sim 1, \ R \sim d^{-2} \ .$$

$$d^2\Phi/dz^2 = d[W - G(1+\alpha_0)d^2W/dz^2] \ .$$

Case IV:

$$R \leq O(d^{-1}), \ RG \sim d^{-2} \ .$$

$$d^2\Phi/dz^2 = -dG(1+\alpha_0)d^2W/dz^2 \ .$$

The regions of (R, G) parameter space covered by these cases are illustrated in Figure 1. In case I, the leading order balance in (4.2) is purely diffusive; we shall show below that there is a second order balance between diffusion and the swimming of the micro-organisms. In case II, the leading order balance is between diffusion and advection of the micro-organisms by the bulk fluid flow, while the balance also includes gyrotaxis due to

vertical shear in the flow in case III. Finally, in case IV, diffusion balances the gyrotactic term alone. We shall restrict attention to cases I, II and IV, although mathematically II is a special case of III, because once again the latter leads to a complicated transcendental eigenvalue problem which itself requires numerical solution.

Case I : $k \sim d$ and $G \leq O(d^{-1})$, $R \sim 1$

Consistent with (4.7), we choose

$$\Phi \sim 1 \ , \ R \sim 1 \ , \ G \sim d^{-1} \ , \ W \sim d$$

and expand Φ, R and W in powers of d, so that

$$\Phi = \sum_{n=o}^{\infty} d^n \Phi_n \ , \quad W = \sum_{n=1}^{\infty} d^n W_n, \ R = \sum_{n=o}^{\infty} d^n R_n \ , \tag{4.8}$$

and we write

$$G = d^{-1} G_{-1} \quad (G_{-1} = O(1)) \ . \tag{4.9}$$

To obtain information about the growth rate in this particular case, we allow σ to be non-zero and, since it turns out that $\sigma \sim d^2$, we expand it as

$$\sigma = \sum_{n=2}^{\infty} d^n \sigma_n \tag{4.10}$$

a priori, for convenience. On substituting (4.8), (4.9) and (4.10) into equations (4.1) and (4.2) and the boundary conditions (3.13), we find at leading order that

$$\frac{d^4 W_1}{dz^4} + \tilde{k}^2 R_0 \Phi_0 = 0 \ , \tag{4.11a}$$

$$\frac{d^2 \Phi_0}{dz^2} = 0 \ , \tag{4.11b}$$

and

$$\frac{d\Phi_0}{dz} = W_1 = \frac{dW_1}{dz} = 0 \text{ at } z = -1, \ 0, \tag{4.11c}$$

while at second order

$$\frac{d^4 W_2}{dz^4} + \tilde{k}^2 R_0 \Phi_1 = -\tilde{k}^2 R_1 \Phi_0 \ , \tag{4.12a}$$

$$\frac{d^2 \Phi_1}{dz^2} = \frac{d\Phi_0}{dz} - G_{-1}(1 + \alpha_0) \frac{d^2 W_0}{dz^2} \ , \tag{4.12b}$$

with boundary conditions

$$\frac{d\Phi_1}{dz} - \Phi_0 = W_2 = \frac{dW_2}{dz} = 0 \text{ at } z = -1, \ 0 \ . \tag{4.12c}$$

The second and higher order systems of equations are inhomogeneous and must satisfy solvability conditions. These conditions are found in the usual manner (Ince, 1956): each system of inhomogeneous equations is multiplied by the adjoint of the homogeneous system and integrated from $z = -1$ to 0, and the resulting integral must vanish. This is equivalent to setting to zero the integral of the cell conservation equation (4.2) over the layer depth.

The solvability condition at $O(d)$ is satisfied identically, independently of σ_2 and R_0, while at $O(d^2)$

$$(\tilde{k}^2 + \sigma_2) \int_{-1}^{0} \Phi_0 dz + \int_{-1}^{0} W_1 dz = 0 \tag{4.13}$$

and at $O(d^3)$

$$(\tilde{k}^2 + \sigma_2) \int_{-1}^{0} \Phi_1 dz + \int_{-1}^{0} W_2 dz$$

$$= G_{-1}[1 + \alpha_0 - (1 - \alpha_0)\tilde{k}^2] \int_{-1}^{0} W_1 dz - \sigma_3 \int_{-1}^{0} \Phi_0 dz - \int_{-1}^{0} z W_1 dz \ . \tag{4.14}$$

The leading order solution is

$$\Phi_0 = 1 \ , \ W_1 = -R_0 \tilde{k}^2 (z^4 + 2z^3 + z^2)/24 \ , \tag{4.15}$$

where Φ_0 has been normalised without loss of generality. Imposing the solvability condition (4.13) gives

$$\sigma_2 = \tilde{k}^2 \left(\frac{R_0}{720} - 1 \right) \ . \tag{4.16}$$

The second order solution is

$$\Phi_1 = z - G_{-1}(1 + \alpha_0) W_1 \ ,$$

$$W_2 = (\frac{\tilde{k}^2 R_0}{40} - \frac{\tilde{k}^2 R_1}{12} - G_{-1}(1 + \alpha_o)\frac{\tilde{k}^4 R_0^2}{360})z^3 + (\frac{\tilde{k}^2 R_0}{60} - \frac{\tilde{k}^2 R_1}{24} - G_{-1}(1 + \alpha_0)\frac{\tilde{k}^4 R_0^2}{560})z^2$$

$$-\frac{\tilde{k}^2 R_0}{120} z^5 - \frac{\tilde{k}^2 R_1 z^4}{24} - G_{-1}(1 + \alpha_0)\frac{\tilde{k}^4 R_0^2}{720}(\frac{z^8}{56} + \frac{z^7}{14} + \frac{z^6}{12}) \ , \tag{4.17}$$

and the solvability condition (4.14) yields

$$\sigma_3 = \frac{\tilde{k}^2 R_1}{720} - \frac{\tilde{k}^2 R_0}{720}[\frac{1}{2} + G_{-1}(1 + \alpha_0)] + \frac{\tilde{k}^4 R_0}{720} G_{-1}[1 - \alpha_0 + \frac{3R_0}{720}\frac{(1 + \alpha_0)}{7}] \ . \tag{4.18}$$

Thus, with this choice of scaling, there is just one solution, the vertical structure of which consists of one bioconvection cell and which we therefore class as mode 1. On the neutral curve $\sigma = 0$ and then

$$R = 720\{1 + d[\frac{1}{2} + G_{-1}(1 + \alpha_0) - 2\tilde{k}^2 G_{-1}(5 - 2\alpha_0)/7]\} + O(d^2) \ . \tag{4.19}$$

Proceeding to the next order, it can be shown that, when $G = 0$, the neutral curve is

$$R = 720\{1 + \frac{1}{2}d + (\frac{13}{105} + \frac{17\tilde{k}^2}{462})d^2\} + O(d^3) \ . \tag{4.20}$$

Thus, in the absence of gyrotaxis, $k = 0$ is a local minimum of the neutral curve and the wavelength of the most unstable mode is infinite (as found by CLS). On the other hand, in the presence of gyrotaxis, (4.19) shows that $k = 0$ is a local *maximum*, since $\alpha_0 < 1$, from which it follows that the most unstable mode must occur at some value of $k > O(d)$, as suggested by observations (e.g. Kessler, 1985). Examples of the neutral curves are given in Figure 2(a) when $d = 0{\cdot}1$, $G = 0,\ 0\cdot 5$ and $\alpha_o = 0{\cdot}2$.

The critical value of G at which $k = 0$ changes from being a minimum to a local maximum of the neutral curve can be found by noting that, if $G = O(1)$, then linearity shows that

$$R = 720\{1 + \frac{d}{2} + d^2[\frac{13}{105} + G(1 + \alpha_0) + \tilde{k}^2(\frac{17}{462} - \frac{2}{7}G(5 - 2\alpha_0))]\} + O(d^3) \tag{4.21}$$

and the critical value of G is

$$G_c = \frac{17}{132(5 - 2\alpha_0)} + O(d) \ . \tag{4.22}$$

Estimates of σ for fixed values of R can be obtained from (4.16) and (4.18), which provide a useful check on numerical calculations, and in particular we note that gyrotaxis introduces a dependence on $\tilde{k}^4$.

The preceding analysis is readily shown to be valid in the limit as $k \to 0$, but not for values of $k >> O(d)$. However it can be extended to the general case when $d,\ k << 1$, by expanding in powers of both d and k^2. This is done in Appendix B, and it shows that on the neutral curve

$$R = 720[1 + \frac{d}{2} + k^2(\frac{17}{462} - \frac{2G}{7}(5 - 2\alpha_0))] + O(d^2, dk^2, k^4) \tag{4.23}$$

(c.f. (4.21)). A special case of this result occurs when

$$d^{\frac{1}{2}} << k << 1 \tag{4.24}$$

and the expansion proceeds in powers of k^2. This is the scheme used by CLS, but their analysis was not strictly valid because k was allowed to tend to zero without regard to the restriction (4.24). Instead, (4.23) shows that

$$R \to 720 \ \text{ as } \ d, k^2 \to 0 \ .$$

The neutral curves given by (4.19), (4.20), (4.21) and (4.23) all show that $k = 0$ is a minimum of the neutral curve when $G < G_c$, and that R decreases monotonically as

k increases when $G > G_c$, provided that d and $k << 1$. Thus, up to the accuracy of the expansion schemes, we conclude that the most unstable wavenumber is $k_c = 0$ when $G < G_c$, and $k_c \geq O(1)$ when $G > G_c$.

The inequalities which define Case I do not specify the scaling uniquely, even when restrictions (4.6) and (4.7) are imposed. However a little analysis shows that the only possible scalings for non-trivial solutions are

$$\Phi \sim 1 \ , \ R \sim 1 \ , \ W \sim d \text{ and } G \leq O(d^{-1}) \tag{4.25}$$

and so there are no other fundamentally different solutions.

Case II: $k \sim d$ **and** $G \leq O(d), R \sim d^{-2}$.

We suppose that $\sigma = 0$,

$$\Phi \sim 1 \ , \ G \sim d \ , \ R \sim d^{-2} \text{ and } W \sim d^{-1} \ , \tag{4.26}$$

and expand the variables in powers of d:

$$\Phi = \sum_{0}^{\infty} d^n \Phi_n \ \ , \ \ W = \sum_{-1}^{\infty} d^n W_n \ , \ R = \sum_{-2}^{\infty} d^n R_n \ , \tag{4.27}$$

and define

$$G_1 = G/d = O(1) \ . \tag{4.28}$$

With these expansions the leading order terms in the governing equations (4.1), (4.2) and (3.13) give

$$\frac{d^4 W_{-1}}{dz^4} + R_{-2} \tilde{k}^2 \Phi_0 = 0 \ , \tag{4.29a}$$

$$\frac{d^2 \Phi_0}{dz^2} - W_{-1} = 0 \tag{4.29b}$$

and

$$d\Phi_0/dz = W_{-1} = dW_{-1}/dz = 0 \text{ at } z = -1, 0 \ . \tag{4.30}$$

Eliminating Φ_0 from (4.29) and (4.30) yields

$$\frac{d^6 W_{-1}}{dz^6} + R_{-2} \tilde{k}^2 W_{-1} = 0 \ , \tag{4.31a}$$

$$W_{-1} = dW_{-1}/dz = d^5 W_{-1}/dz^5 = 0 \text{ at } z = -1, 0 \ . \tag{4.31b}$$

Equation (4.31a) has solutions

$$\begin{aligned} W_{-1} =& A \cos(\omega z) + B \sin(\omega z) + \exp(\omega z \sqrt{3}/2)[C \cos(\omega z/2) \\ &+ D \sin(\omega z/2)] + \exp(-\omega z \sqrt{3}/2)[E \cos(\omega z/2) + F \sin(\omega z/2)] \ , \end{aligned} \tag{4.32}$$

where

$$\omega^6 = R_{-2}\tilde{k}^2 \ . \tag{4.33}$$

A, B, C, D, E and F are constants determined by applying the boundary conditions (4.31b), and for a non-zero solution ω must satisfy the eigenvalue problem

$$\sin(\omega/2) = 0 \tag{4.34a}$$

or

$$\cos(\omega/2)\cosh^2(\omega\sqrt{3}/2) - 2\cosh(\omega\sqrt{3}/2)$$
$$+2\cos(\omega/2) - \cos^3(\omega/2) = 0 \ . \tag{4.34b}$$

The roots of (4.34a) are $\omega = 2m\pi$ $(m = 1, 2, ...)$. For large values of ω, equation (4.34b) is dominated by exponentially large terms and must have roots at $\cos(\omega/2) \simeq 0$ which suggests that (4.34b) has roots

$$\omega \simeq (2m' + 1)\pi \quad (m' = 0,\ 1,\ 2, ...) \ . \tag{4.35}$$

In fact, it easily checked numerically that there is no root corresponding to $m' = 0$, but that for $m' = 1$ (4.35) is already accurate to within 1% and becomes successively better for greater values of m'. So for a non-trivial solution ω takes values

$$\omega_2 = 2\pi \ , \ \omega_3 \simeq 3\pi \ , ... \ .$$

At this point, we have multiple solutions to the linear stability problem. Corresponding to the roots ω_2, ω_3 ,..., there are *branches* of the neutral curve $R^{(2)}(k)$, $R^{(3)}(k), ...$ given by (4.33). We must also examine the structure of the vertical velocity field $W(z)$ to determine the mode or type of solution. A solution is said to be *mode* n if $W(z)$ changes sign $(n-1)$ times for $-1 < z < 0$. In other words mode n $(n = 1, 2, ...)$ consists of n layers of convection cells stacked vertically one above the other throughout $-1 < z < 0$ (see §3).

The neutral curve of the smallest root ω_2 is given by (4.32) as

$$R^{(2)} = (2\pi)^6/d^2\tilde{k}^2 + O(d^{-1}) \simeq 6{\cdot}15 \times 10^4/d^2\tilde{k}^2 + O(d^{-1}) \ ,$$

and the constants $A, ..., F$ can be calculated for this branch to show that

$$W_{-1} \propto \sin\pi z[\sinh(\pi\sqrt{3})\cos(\pi z) - \cosh(\pi\sqrt{3}/2) \times \sinh(\pi[z + \tfrac{1}{2}]\sqrt{3})]$$

which is antisymmetric about $z = -\frac{1}{2}$ and is therefore mode 2.

In Case II, the only alternatives to the choice of scales (4.28), which are consistent with (4.6) and (4.7), are of the form

$$\Phi \sim 1, \ R \sim d^{-2}, \ W \sim d^{-1} \text{ and } G \sim d^m (m = 2, 3, ...) \ .$$

Since G_1 does not appear in the leading order problem (4.29), the alternative choices of scaling in which G is of smaller magnitude will not change the nature of the leading order solution, but just make refinements at higher orders.

In order to interpret the results of Cases I and II, we suppose without loss of generality that (4.7) holds and ask what solutions are possible for a given value of G. It is clear from the preceding paragraph and from (4.27) that for $G \leq O(d)$, Cases I and II both provide solutions. Case I gives the $R^{(1)}$ branch corresponding to mode 1, and Case II provides the higher branches and modes. This is summarised in Figure 1 and at the top of Table 1. Also, when $G \sim 1$, Cases I and III both provide solutions. Although, as mentioned previously, Case III has not been completely analysed analytically, it is reasonable to expect that again Case I gives the $R^{(1)}$ branch and Case III gives the higher branches $R^{(n)} \sim d^{-2}$.

Case IV: $k \sim d$ **and** $R \leq O(d^{-1})$, $RG \sim d^{-2}$

As in Case I, we analyse the shallow layer approximation to the governing equations in the limit of small wavenumbers. Because of the complicated nature of the eigenvalue problem which arises here, we exclude the possibility of oscillatory solutions on the neutral curves, in the more detailed calculations, by setting $\sigma = 0$. Possible scalings are of the form

$$\Phi \sim 1 \ , \ G \sim d^{-m} \ , \ R \sim d^{m-2} \ , \ W \sim d^{m-1} \ (m = 1, 2, ...) \ , \tag{4.36}$$

and the problem subdivides naturally into the three cases $m = 1, m = 2$ and $m \geq 3$. When $m = 1$, $G \sim d^{-1}$ and we have already demonstrated that Case I provides a mode 1 solution when $G \sim d^{-1}$. Thus we might anticipate that the new scaling yields the higher order modes by analogy with Case II. Moreover when $m \geq 2$, we shall show that Case IV gives *all* the solution branches, including the mode 1 solution. What is more unexpected is that when $m = 2$ and G exceeds a critical value, the solution for the lowest branch breaks down at small wavenumbers. We conjecture that in this case oscillatory solutions exist and we shall indicate an appropriate scaling for such solutions.

We begin by setting $m = 2$ and define

$$\Phi = \sum_{0}^{\infty} d^n \Phi_n \ , \ W = \sum_{1}^{\infty} d^n W_n \ , \ R = \sum_{0}^{\infty} d^n R_n \text{ and } G = d^{-2} G_{-2} \ , \tag{4.37}$$

which is consistent with (4.6) and (4.7). Expressions (4.37) are substituted into equations (4.1), (4.2) and (3.13), and at leading order

$$\frac{d^4 W_1}{dz^4} + \tilde{k}^2 R_0 \Phi_0 = 0 \ , \tag{4.38a}$$

$$\frac{d^2}{dz^2}[\Phi_0 + G_{-2}(1 + \alpha_0) W_1] = 0 \tag{4.38b}$$

subject to the boundary conditions

$$\frac{d\Phi_0}{dz} = W_1 = \frac{dW_1}{dz} = 0 \text{ on } z = -1, 0 \ . \tag{4.38c}$$

This system of equations has the solution

$$\Phi_0 = G_{-2}(1 + \alpha_0)(K - W_1) \ ,$$

$$W_1 = A \cos \omega z + B \sin \omega z - (A + K) \cosh \omega z - B \sinh \omega z + K \ , \tag{4.39}$$

where

$$\omega^4 = \tilde{k}^2 R_0 G_{-2}(1 + \alpha_0) \tag{4.40}$$

and A, B and K are constants which satisfy

$$\begin{pmatrix} \cos\omega - \cosh\omega & \sinh\omega - \sin\omega \\ \sinh\omega + \sin\omega & \cos\omega - \cosh\omega \end{pmatrix} \begin{pmatrix} A \\ B \end{pmatrix} = K \begin{pmatrix} \cosh\omega - 1 \\ -\sinh\omega \end{pmatrix} . \tag{4.41}$$

This equation can in principle be solved (for $A/K, B/K$) for any value of ω save that for which the matrix on the left hand side is singular, in which case $K = 0$.

The boundary conditions on Φ_0 to this order are degenerate and we proceed to the next order, $O(d)$, to find an additional constraint on Φ_0 arising from the solvability condition. Similarly, there is an additional constraint on Φ_1 at $O(d^2)$, and so on to higher orders. As in Case I, the solvability condition is found by integrating the cell conservation equation over the layer depth. It turns out that the solvability condition is satisfied identically at $O(d)$, but at $O(d^2)$ it is easily shown that

$$\tilde{k}^2 \int_{-1}^{0} \Phi_0 dz = \int_{-1}^{0} \left\{ \frac{z^2}{2} G_{-2}(1+\alpha_0)(d^2 W_1/dz^2) - (G_{-2}(1-\alpha_0)\tilde{k}^2 + 1) W_1 \right\} dz$$

which implies that

$$\int_{-1}^{0} W_1 dz = -F(\tilde{k}; G_{-2}, \alpha_0) K \ , \tag{4.42}$$

where

$$F(\tilde{k}; G_{-2}, \alpha_0) = \frac{G_{-2}(1+\alpha_0)\tilde{k}^2}{1 + G_{-2}(1-\alpha_0)\tilde{k}^2 - G_{-2}(1+\alpha_0)(\tilde{k}^2+1)} \ , \tag{4.43}$$

using the leading order solution (4.39). Evaluating the integral in (4.42) and incorporating (4.41), the conditions on A, B and K can be written as

$$\begin{pmatrix} \cos\omega - \cosh\omega & \sinh\omega - \sin\omega & 1 - \cosh\omega \\ \sinh\omega + \sin\omega & \cos\omega - \cosh\omega & \sinh\omega \\ \sin\omega - \sinh\omega & \cos\omega + \cosh\omega - 2 & \omega - \sinh\omega + F \end{pmatrix} \begin{pmatrix} A \\ B \\ K \end{pmatrix} = 0 \ , \tag{4.44}$$

which is an eigenvalue problem for ω, and hence for R. Equation (4.44) has a non-trivial solution if and only if

$$\omega(1+F)(1 - \cos\omega\cosh\omega) = 2[\sinh\omega(1-\cos\omega) + \sin\omega(1-\cosh\omega)] \ . \tag{4.45}$$

The roots of (4.45) and the corresponding solutions (4.39) are discussed in detail in Appendix C. There is a set of even roots, associated with even modes, given by

$$\omega_{2m'} \simeq (4m'+1)\pi/2 \quad (m' = 1,\ 2, ...)$$

independently of the value of F. The odd roots do depend on F and, when $G_{-2}(1+\alpha_0) < 1$, there is also a set of odd roots with associated odd modes such that

$$0 \leq \omega_1 \leq \omega_2 \leq \omega_3 \leq \ldots \ .$$

The most unstable branch is

$$R^{(1)} = \omega_1^4 / k^2 G(1+\alpha_0) + O(d) \tag{4.46}$$

and mode 1 is the preferred mode. When $\tilde{k} >> 1$, $\omega_1 \simeq 3\pi/2$ and therefore $R^{(1)} \propto k^{-2}$ so that disturbances of shorter wavelengths are more unstable than those of longer wavelengths. The behaviour of $R^{(1)}$ as $\tilde{k} \to 0$ can be calculated by expanding (4.45) in a Taylor series about $\omega = 0$ which shows that

$$\omega_1^4 \simeq \frac{720 G_{-2}(1+\alpha_0)\tilde{k}^2}{1 - G_{-2}(1+\alpha_0)} \quad (0 < \tilde{k} << 1\ ,\ \ G_{-2}(1+\alpha_0) < 1)$$

(see Appendix D) so that

$$R^{(1)} \to 720/[1 - G_{-2}(1+\alpha_0)] \text{ as } \tilde{k} \to 0\ . \tag{4.47}$$

The roots ω_n $(n > 1)$ do not tend to 0 as $\tilde{k}$ tends to 0, so

$$R^{(n)} \sim \tilde{k}^{-2} \to \infty \text{ as } \tilde{k} \to 0 \tag{4.48}$$

for $n > 1$.

Hurle et al. (1967) considered the Bénard problem with boundaries of finite conductivity and were able to show that, in the limit of perfectly insulating boundaries, the Rayleigh number of the lowest, odd mode tends to 720 as the wavenumber tends to zero, and the Rayleigh number of the first even mode tends to ∞ as the wavenumber tends to zero. Thus the unusual contrast between the behaviour of $R^{(1)}$ given by (4.47) and that of the higher branches given by (4.48) has a parallel in Bénard convection. Indeed this comparison was noted by CLS but, when gyrotaxis is included in the analysis, $\tilde{k} = 0$ is a local *maximum* of the neutral curve $R^{(1)}$ both in this case (which we shall demonstrate later numerically) and in Case I, whereas CLS, and Hurle et al. (1967), found that $\tilde{k} = 0$ was in all cases a local *minimum*.

It can be shown that there is a critical value of F, $F_c \simeq -0.75$, such that the root ω_1 does not exist when $F_c < F < 0$. When $G_{-2}(1+\alpha_0) < 1$, F always lies outside $(-1, 0)$, but when $G_{-2}(1+\alpha_0) > 1$ and $\tilde{k}$ is sufficiently small, $F_c < F < 0$ and the branch $R^{(1)}$ corresponding to mode 1 does not exist.

We now consider the other possible scalings given by (4.36), and the analysis hinges on the solvability condition (4.42). It is readily seen that when $m = 1$, and the variables are expanded in powers of d accordingly, solvability requires simply that

$$\int_{-1}^{0} W_0 dz = 0\ ,$$

while if $m \geq 3$, the solvability condition becomes

$$\int_{-1}^{0} W_{m-1} dz = \frac{(1+\alpha_0)\tilde{k}^2 K}{(1+\alpha_0) + 2\alpha_0 \tilde{k}^2}\ .$$

Suppose firstly, that $m = 1$: the analysis proceeds as before, when $m = 2$, but with F now set to zero, and we conclude that ω_1 does not exist for any values of $\tilde{k}$, i.e. the most unstable mode when $m = 1$ is mode 2.

(see Table 2), so that overstability is unlikely to be found in such a suspension, but as discussed later it is possible that overstability could be found in suspensions of different species of micro-organisms.

We conclude the shallow layer analysis with the following observations. For small wavenumbers, $k \sim d$, and when $G = O(1)$, mode 1 is the most unstable mode and the neutral curve has a local minimum at $k = 0$. As G increases to $O(d^{-1})$, $k = 0$ becomes a local maximum. It can also be shown that $R^{(1)} \sim k^2$ as $k \to \infty$ when $G = O(d^{-1})$ (see Appendix E), so that $R^{(1)}$ must have a global minimum when $k \geq O(1)$. This leads to a prediction of a critical wavelength for instability which is finite. Finally, for large values of $G \geq O(d^{-2})$, oscillatory modes are found.

4.2 Deep layer approximation, $d >> 1$

When $d >> 1$ the exponential profile of the equilibrium solution gives a boundary layer at the upper surface containing a high concentration of cells. Variables are therefore expanded in inverse powers of d and the method of matched asymptotic expansions is used to resolve the boundary layer. From equations (3.12) and (3.13), we expect Φ to be exponentially small in the outer region, away from the upper boundary layer, where $z = O(1)$. The numerical results of §5 suggest that for oscillatory solutions, which are found for certain parameter values, $\mathrm{Im}(\sigma) = O(d^2)$ and should therefore be found in the leading order terms of the asymptotic analysis in the boundary layer. However, attempts at a suitable scaling to achieve such a balance have been unsuccessful, as we describe below. Thus the following analysis is restricted to cases where $\sigma = O(1)$, in which case it is shown that σ is always real. For clarity, we first consider neutral curves, on which $\mathrm{Re}(\sigma) = 0$, and suppose that $\mathrm{Im}(\sigma) = 0$ also.

When $d >> 1$, the governing linear stability equations (3.11) to (3.13) in the outer region become

$$\Phi = 0$$

and

$$(\frac{d^2}{dz^2} - k^2)^2 W(z) = 0 \tag{4.51}$$

subject to boundary conditions

$$W = dW/dz = 0 \text{ on } z = -1 \tag{4.52}$$

and matching conditions as $z \to 0$. The general solution of (4.51) and (4.52) is

$$W = -kA(z+1)\cosh[k(z+1)] + [A + B(z+1)]\sinh[k(z+1)]$$

where constants A and B can be expanded in powers of d, e.g.

$$A = A_0 + d^{-1}A_{-1} + d^{-2}A_{-2} + \ldots .$$

In the inner region, define

$$z_I = dz = O(1) \text{ and } D_I \equiv d/dz_I ,$$

in terms of which the equations become

$$(D_I^2 - d^{-2}k^2)^2 W = -d^{-5} R k^2 \Phi \ , \tag{4.53a}$$

$$(D_I^2 - D_I - d^{-2}k^2)\Phi = -d\exp(z_I)[G(1+\alpha_0)D_I^2 - G(1-\alpha_0)d^{-2}k^2 - d^{-2}]W \tag{4.53b}$$

and

$$(D_I - 1)\Phi = W = D_I W = 0 \text{ at } z_I = 0$$

with matching conditions as $z_I \to -\infty$. As in the shallow layer approximation, there are several balances possible between the terms in (4.53) but the presence of the exponential term in (4.53b) makes the analysis more difficult and we restrict attention to the case when

$$G \leq O(d^{-2}) \text{ and } W \sim d^{-1} \text{ as } d \to \infty$$

which covers the parameter range of interest in experiments, as will be discussed later (see also Table 2). In particular we define

$$W = \sum_1^\infty d^{-n} W_{-n} \ , \quad \Phi = \sum_0^\infty d^{-n} \Phi_{-n} \ ,$$

$$R = \sum_{-4}^\infty d^{-n} R_{-n} \text{ and } G = d^{-2} G_{-2} \ , \tag{4.54}$$

where $\Phi \sim 1$ as in (4.7). Again for buoyancy to drive the flow, the magnitude of the right hand side of (4.53a) must balance the largest term on the left hand side.

Substituting the expansions (4.54) into (4.53) gives at leading order

$$D_I^4 W_{-1} + R_4 k^2 \Phi_0 = 0 \ ,$$

$$D_I(D_I - 1)\Phi_0 = 0 \ ,$$

and at second order

$$D_I^4 W_{-2} + R_4 k^2 \Phi_{-1} = -R_3 k^2 \Phi_0 \ ,$$

$$D_I(D_I - 1)\Phi_{-1} = 0 \ .$$

The leading order equations show that the balance in the cell conservation equation is between diffusion and the up-swimming of the micro-organisms.

The first and second order solutions, when the boundary conditions at $z_I = 0$ have been imposed, are

$$W_{-1} = z_I^2(\alpha_{-1} z_I + \beta_{-1}) + k^2 R_4(1 + z_I - \exp(z_I)) \ ,$$
$$\Phi_0 = \exp(z_I)$$

and

$$W_{-2} = z_I^2(\alpha_{-2} z_I + \beta_{-2}) + k^2 R_3(1 + z_I - \exp(z_I))$$
$$\Phi_{-1} = 0 \ ,$$

where α_{-1}, β_{-1}, α_{-2} and β_{-2} are constants. When the inner and outer solutions are matched in the usual manner (see e.g. Kevorkian & Cole, 1981), it can be shown that there is a non-trivial solution if and only if

$$(A_0 + B_0)\sinh k - kA_0 \cosh k = \alpha_{-1} = \alpha_{-2} = \beta_{-1} = 0 \ .$$

The Rayleigh number, R_4, is determined from the solvability condition on the inner system of equations by integrating the cell conservation equation at third order from $z_I = -\infty$ to 0. This gives

$$R_4 = 2/[1 - G_{-2}(1 + \alpha_0)] \ , \tag{4.55}$$
$$A_0 = -\frac{k^2 R_4 \sinh k}{\sinh^2 k - k^2} \ ,$$
$$B_0 = -k^2 R_4 (k \cosh k - \sinh k)$$

and

$$\beta_{-2} = k^3 R_4 (\sinh k \cosh k - k)/(\sinh^2 k - k^2) \ .$$

Equation (4.55) is valid provided that

$$G_{-2} = d^2 G < (1 + \alpha_0)^{-1} \ , \tag{4.56}$$

and it is reasonable to suppose that if (4.56) does not hold then oscillatory solutions may exist, and an asymptotic analysis based on a scaling in which $\sigma = O(d^2)$ is required. To find the dependence of R on the wavenumber k, the inner solvability condition at fourth order implies that

$$R_3 = 4R_4 \beta_{-2}/k^2 \ ,$$

so that

$$R = \frac{2d^4}{1 - d^2 G(1 + \alpha_0)} \left\{ 1 + 4d^{-1} \frac{k(\sinh k \cosh k - k)}{\sinh^2 k - k^2} + O(d^{-2}) \right\} \ . \tag{4.57}$$

R_3 is a monotonically increasing function of k and it is readily shown that the above analysis is valid in the limit as k tends to zero. Thus the critical wavenumber predicted by this analysis is zero, provided that (4.56) holds and $k \leq O(1)$. However the numerical solutions of §5 show that for values of G larger than some critical value G_c, the most unstable wavelength is $O(d)$, giving convection cells of a horizontal wavelength commensurate with the sublayer depth ℓ. When $d = 40.0$ and $\alpha_0 = 0$, then $0.7 < d^2 G_c < 0.8$ but the asymptotic analysis does not predict G_c, unlike the shallow layer case, suggesting that d has to be very large for good agreement.

A calculation similar to that leading to (4.57), using the same inner and outer variables, gives the growth rate $\sigma(R, k)$ when $\sigma = O(1)$, and after some algebra it can be shown that

$$\sigma = k^2 \left(\frac{R - R(k)}{R(k)} \right) + O(d^{-1}\delta, d^{-2}) \ , \tag{4.58}$$

where $R(k)$ is the neutral curve given by equation (4.57). In this case σ is real and so the solution is stationary. Equation (4.58) has been derived from a more complicated transcendental equation by expanding in a Taylor series in powers of

$$\delta = \frac{R - R(k)}{R(k)S_c} ,$$

which is assumed to be small, given $S_c \simeq 20$ in the experiments.

The possible balances between terms in the solvability conditions can be examined to show that the neutral curve is given by an expression of the form of (4.57) wherever G satisfies (4.56). The full leading order solution (i.e. combining the inner and outer solutions) can be shown to be mode 1.

Returning to the question of oscillatory solutions when $\mathrm{Im}(\sigma) = O(d^2)$, it is straight forward to show that the scaling in (4.54) leads only to the trivial solution unless both $\mathrm{Im}(\sigma) = 0$ and $\sigma \leq O(1)$. It appears that terms on the right hand side of (4.53b) are required at leading order to find a non-trivial solution, but such a scaling yields an ordinary differential equation with exponential coefficients which we have been unable to solve analytically.

Appendix B

Suppose that $d, k^2 << 1$ and $G = O(1)$ in Case I of §4.1 and consider the shallow layer equations (4.1) and (4.2), with boundary conditions (3.13). We expand the variables in powers of both d and k^2, and write

$$\Phi = \tilde{\Phi}_0 + d\tilde{\Phi}_{1,0} + k^2\tilde{\Phi}_{0,1} + d^2\tilde{\Phi}_{2,0} + dk^2\tilde{\Phi}_{1,1} + k^4\tilde{\Phi}_{0,2} + ...,$$

$$W = d^{-1}k^2\tilde{W}_{-1,1} + k^2\tilde{W}_{0,1} + d^{-1}k^4W_{-1,2} + dk^2\tilde{W}_{1,1} + k^4\tilde{W}_{0,2} + d^{-1}k^6\tilde{W}_{-1,3} + \dots ,$$

$$R = \tilde{R}_0 + d\tilde{R}_{1,0} + k^2\tilde{R}_{0,1} + \dots ,$$

and

$$\sigma = k^2\tilde{\sigma}_{0,1} + dk^2\tilde{\sigma}_{1,1} + k^4\tilde{\sigma}_{0,2} + \dots .$$

These expansions are substituted into the governing equations (written in terms of k rather than $\tilde{k}$) and systems of ordinary differential equations are derived at $O(1)$, $O(d)$, $O(k^2), \dots$. These are solved to give

$$\Phi = 1 + dz + k^2\frac{\tilde{R}_0 z^2}{720}\left[\frac{1}{2} - \frac{5z^2}{2} - 3z^3 - z^4 + 30G(1+\alpha_0)(z^2+2z+1)\right] + O(d^2, dk^2, k^4) ,$$

$$W = -\frac{\tilde{R}_0}{24}z^2(z^2+2z+1) + d\left[\frac{\tilde{R}_0 z^2}{120}(2+3z-z^3) - \frac{\tilde{R}_{1,0}}{24}z^2(1+2z+z^2)\right]$$

$$+k^2\left[(-2+\frac{\tilde{\sigma}_{0,1}}{S_c})\frac{\tilde{R}_0}{720}z^2\frac{(2z^4+6z^3+5z^2-1)}{2}\right.$$

$$+\frac{\tilde{R}_0^2}{720^2}z^2\frac{(2z^8+10z^7+15z^6-14z^4-20z-13)}{14}$$

$$\left.-\frac{\tilde{R}_0^2}{720^2}z^2G(1+\alpha_0)\frac{30(3z^6-12z^5-14z^4-14z-9)}{7} - \frac{\tilde{R}_{0,1}}{24}z^2(z^2+2z+1)\right] + O(d^2, dk^2, k^4),$$

where the solvability conditions at $O(k^2)$, $O(dk^2)$ and $O(k^4)$ yield

$$\tilde{\sigma}_{0,1} = \frac{\tilde{R}_0}{720} - 1 ,$$

$$\tilde{\sigma}_{1,1} = \frac{1}{720}(-\frac{\tilde{R}_0}{2} + \tilde{R}_{1,0})$$

and

$$\tilde{\sigma}_{0,2} = -\frac{(2+\tilde{\sigma}_{0,1}/S_c)}{42}\frac{\tilde{R}_0^2}{720} + \frac{\tilde{R}_0}{720^2}(\frac{5}{462} + \frac{3G(1+\alpha_0)}{7}) + \frac{\tilde{R}_0}{720}G(1-\alpha_0) + \frac{\tilde{R}_{0,1}}{720} .$$

Setting $\sigma = 0$ gives the neutral curve (4.23).

Appendix C

Here we consider in detail the solution of the eigenvalue problem of Case IV in §4 given by equations (4.39), (4.43)-(4.45). Because this analysis is complicated, we proceed in several stages.

(a) Roots of (4.45)

(i) Even roots:
Equation (4.45) has one set of roots which satsify

$$1 - \cos\omega \cosh\omega = 0, \ \sin\omega > 0 \ , \qquad (C1)$$

independently of the value of F. We write these roots as $0 < \omega_2 < \omega_4 < ...$ with corresponding branches of the neutral curve $R^{(2)}$, $R^{(4)}$... , given by (4.40). These give solutions of mode 2, mode 4, etc. because, at these values of ω, K in (4.39) is zero and

$$W_1 = A\left\{\cos\omega z - \cosh\omega z + (\frac{\cos\omega - \cosh\omega}{\sin\omega - \sinh\omega})\ (\sin\omega z - \sinh\omega z)\right\} \ , \qquad (C2)$$

where A is an arbitrary constant, so that $W_1(-\frac{1}{2}) = 0$, and the solutions (C2) are antisymmetric about $z = -\frac{1}{2}$. Thus (C2) gives even modes. We can readily estimate the eigenvalues of the even modes since $\cosh\omega$ grows exponentially as ω increases. To an error of less than 1%,

$$\omega_2 = 5\pi/2$$

and in general

$$\omega_{2n} \simeq (4n+1)\pi/2 \quad (n = 1, 2, ...) \ .$$

These roots are shown as straight lines parallel to the F-axis in Figure 11.

(ii) Odd roots:
The values of the odd roots of (4.45) depend explicitly on the value of F, given by (4.43). When $|F| >> 1$, the odd roots satisfy

$$1 - \cos\omega \cosh\omega \simeq 1 \ , \ \sin\omega < 0 \ , \qquad (C3)$$

so that $\omega \simeq 3\pi/2, \ 7\pi/2, \ 11\pi/2, ...$ in the limits as $F \to \pm\infty$. The behaviour of the first three odd roots ω_1, ω_3 and ω_5 as F varies is shown in Figure 11. In particular, for values of F between -1 and 0, the loci of the odd roots cross those of the even roots, as do the corresponding branches of the neutral curves. In addition, the root ω_1 vanishes when $F_c < F < 0$, where $F_c \simeq -0{\cdot}75$. To interpret these results, we need to discover how F varies as a function of G_{-2}, α_0 and $\tilde{k}$, and to find the mode of the solution for a given value of ω.

(b) Values of $F(G_{-2},\ \alpha_0,\ \tilde{k})$

The values of F, defined by equation (4.43) are sketched in Figure 12 for the two cases $G_{-2}(1+\alpha_0) \lessgtr 1$. When $G_{-2}(1+\alpha_0) < 1$, F does *not* take values in $[-1, 0]$ and is singular at a critical value of $\tilde{k}$ given by

$$\tilde{k}_c^2 = [1 - G_{-2}(1+\alpha_0)]/2G_{-2}\alpha_0 \ .$$

Thus in this case, the loci of the odd modes do not cross those of the even modes for any valaues of k. Moreover, since

$$\omega_{2n-1}(F = +\infty) = \omega_{2n-1}(F = -\infty) \quad (n = 1, 2, ...) \ ,$$

there is no discontinuity in the valaue of ω as $\tilde{k}$ passes through $\tilde{k}_c$.

When $G_{-2}(1+\alpha_0) > 1$, F is finite and negative for all values of $\tilde{k}$, and takes values between -1 and 0 for sufficiently small wavenumbers so that the crossing of roots does occur and the branch corresponding to ω_1 is not found.

(c) Modes

The structure of $W_1(z)$ does not depend explicitly on the value of F, but only on the value of ω, because when (4.45) is satisfied, the matrix in (4.44) is of rank two and the eigenvector $(A_0,\ B_0,\ K_0)^T$ can be determined from the top two rows of the matrix (apart from a normalisation factor). So, given a value of ω, $W_1(z)$ can be found from (4.39) and (4.44). The results of such calculations are summarized in Figure 11. Even modes are found only when $\omega = \omega_2,\ \omega_4, ...$, while mode 1 is found wherever $\omega < \omega_2$. Higher odd modes are found when $\omega > \omega_2$ as indicated in the figure. Also found are 'wavy' modes 1(3), 3(5), 1(5) etc. The first digit indicates the number of convection cells stacked vertically on top of one another in $-1 < z < 0$, while the digit in parentheses indicates the total number of extrema in the $W_1(z)$ field. Examples of these and other modes are given in Figure 13.

In conclusion, when $G_{-2}(1+\alpha_0) < 1$, there are solution branches $R^{(1)},\ R^{(2)}, ...$ corresponding to modes $1, 2, ...$ for all values of $\tilde{k}$, mode 1 being the most unstable for any particular value of $\tilde{k}$. However when $G_{-2}(1+\alpha_0) > 1$, the branch $R^{(1)}$ is not found at sufficiently small values of $\tilde{k}$, and then $R^{(2)}$ is the most unstable branch, corresponding to mode 2.

Appendix D

Derivation of Equation (4.47)

Equation (4.45) is expanded in powers of $\omega(0 < \omega << 1)$ to give

$$(1+F)(\frac{\omega^5}{6} - \frac{2\omega^9}{7!}) = \frac{\omega^5}{6} - \frac{5\omega^9}{6 \times 7!} + O(\omega^{13})$$

which implies that

$$\omega_1^4 = \frac{F \times 7!}{7 + 12F} + O(\omega^8) \qquad (D1)$$

which is consistent provided that $0 \leq F << 1$. When (4.43) is substituted into (D1), we find that

$$\omega_1^4 \to \frac{720 G_{-2}(1+\alpha_0)\tilde{k}^2}{1 - G_{-2}(1+\alpha_0)} \text{ as } \tilde{k} \to O \ ,$$

provided that $G_{-2}(1+\alpha_0) < 1$, and (4.47) follows directly from (4.40).

Appendix E

Shallow Layer Analysis when $k = O(1)$

With $k = O(1)$ and $\sigma = 0$ the shallow layer approximation to the governing equations is

$$(\frac{d^2}{dz^2} - k^2)^2 W = -d^{-1} R k^2 \Phi \ ,$$

$$(\frac{d^2}{dz^2} - d\frac{d}{dz} - k^2)\Phi = d(1 + dz + ...)[1 - G(1 + \alpha_0)\frac{d^2}{dz^2} + k^2 G(1 - \alpha_0)]W$$

so that when

$$\Phi, W, dG, \text{ and } d^{-1}R = O(1) \ ,$$

the leading order problem is

$$(\frac{d^2}{dz^2} - k^2)^2 W = -d^{-1} R k^2 \Phi \ ,$$

$$(\frac{d^2}{dz^2} - k^2)(\Phi + dG(1 + \alpha_0)W) = 0 \ ,$$

subject to boundary conditions

$$d\Phi/dz = W = dW/dz = O \text{ on } z = -1, 0 \ .$$

The general solution is

$$\Phi = -dGW \ ,$$
$$W = A\cosh(\omega_+ z) + B\sinh(\omega_+ z) + C\cosh(\omega_- z) + D\sinh(\omega_- z)$$

where

$$\omega_\pm^2 = k^2 \pm k\sqrt{RG(1 + \alpha_0)} \ .$$

Application of the boundary conditions yields the following eigenvalue problem for $\omega_\pm$:

$$\omega_-[1 - \cosh(\omega_+)\cosh(\omega_-)] + k\sinh(\omega_+)\sinh(\omega_-) = 0 \ .$$

In general, this last equation has to be solved numerically, but in the limit as $k \to \infty$,

$$R \to 2k^2/G(1 + \alpha_0) \ .$$

Figure Captions

Figure 11

Plots of the eigenvalues $\omega_n(F)$ in Case IV. (See Appendix C.)

Figure 12

Sketches of the function F defined in (4.43):

(a) $d^2G(1+\alpha_0) < 1$; $\tilde{k}_c^2 = [1 - d^2G(1+\alpha_0)]/2d^2G\alpha_0$; and

(b) $d^2G(1+\alpha_0) > 1$.

(See Appendix C.)

Figure 13

Graphs of the vertical velocity field $W(z)$ in Case IV for different values of ω, showing the different modes which are found:

(a) $\omega = 4{\cdot}50$ — mode 1,
(b) $\omega = 7{\cdot}85$ — mode 2,
(c) $\omega = 13{\cdot}50$ — mode 1(3).

(See Appendix C.)

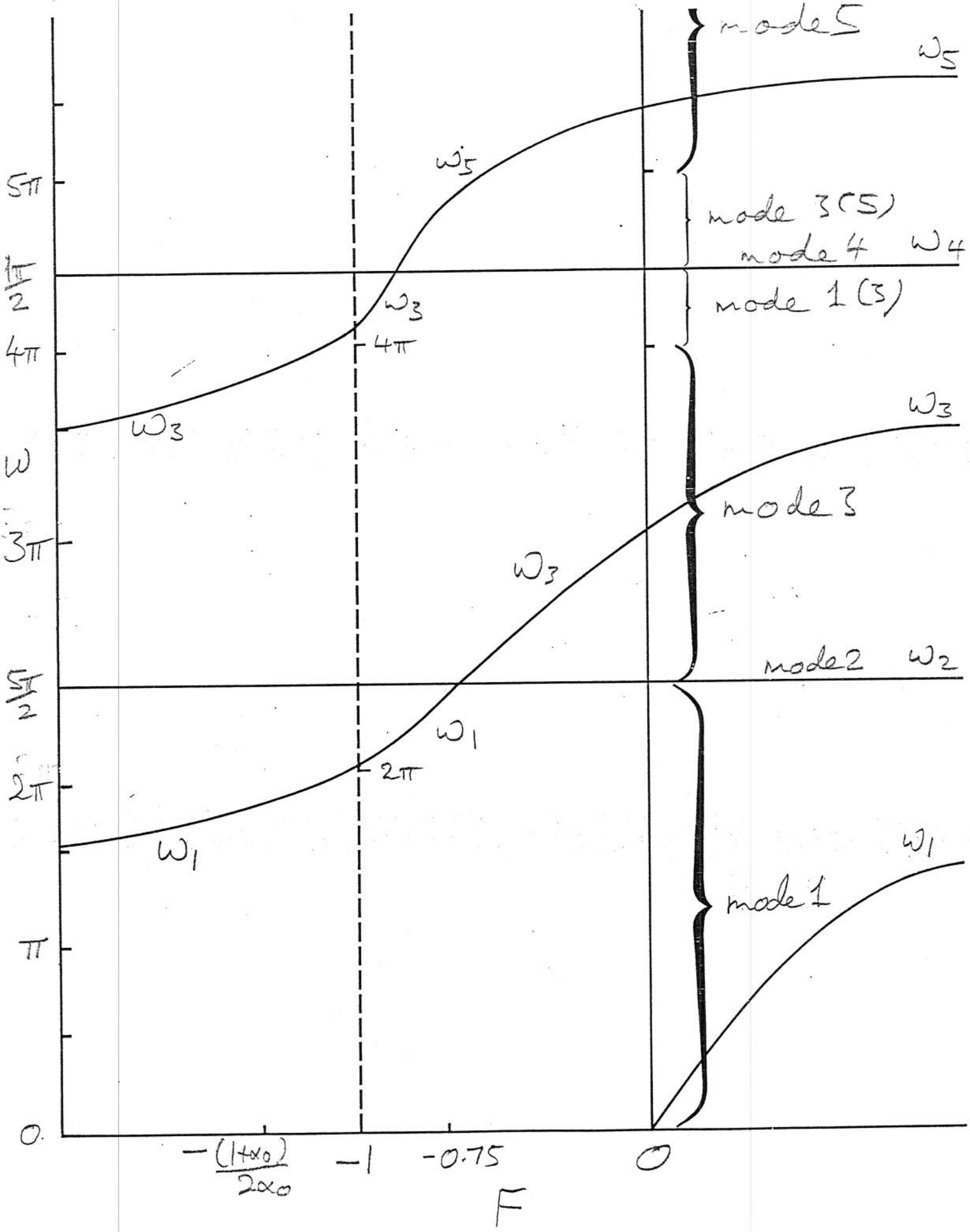
mode 5
ω_5
ω_5
5π
mode 3 (5)
mode 4
ω_4
$\frac{4\pi}{2}$
ω_3
mode 1 (3)
4π
4π
ω_3
ω_3
ω
mode 3
3π
ω_3
mode 2
ω_2
$\frac{5\pi}{2}$
ω_1
2π
2π
ω_1
ω_1
mode 1
π
0
$-\frac{(1+\alpha_0)}{2\alpha_0}$
-1
-0.75
0
F

Figure 11

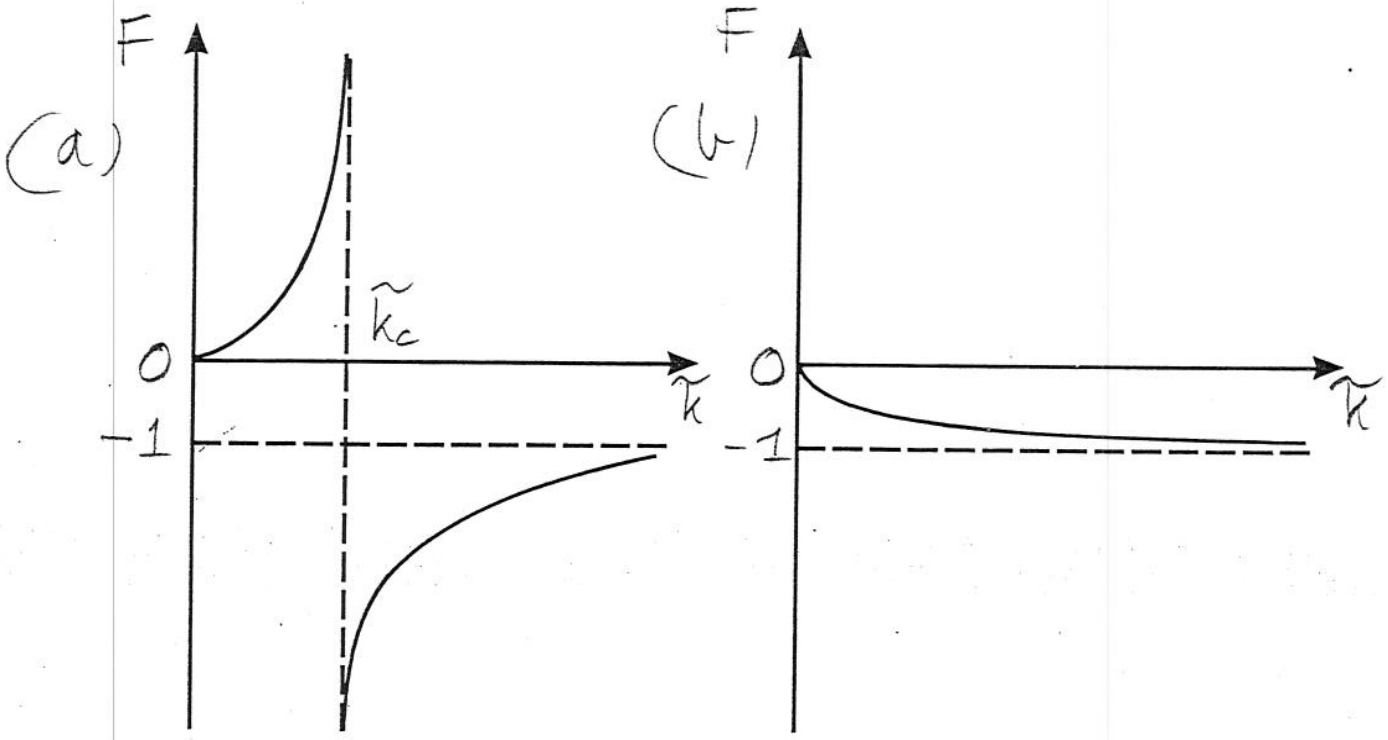

Figure 12

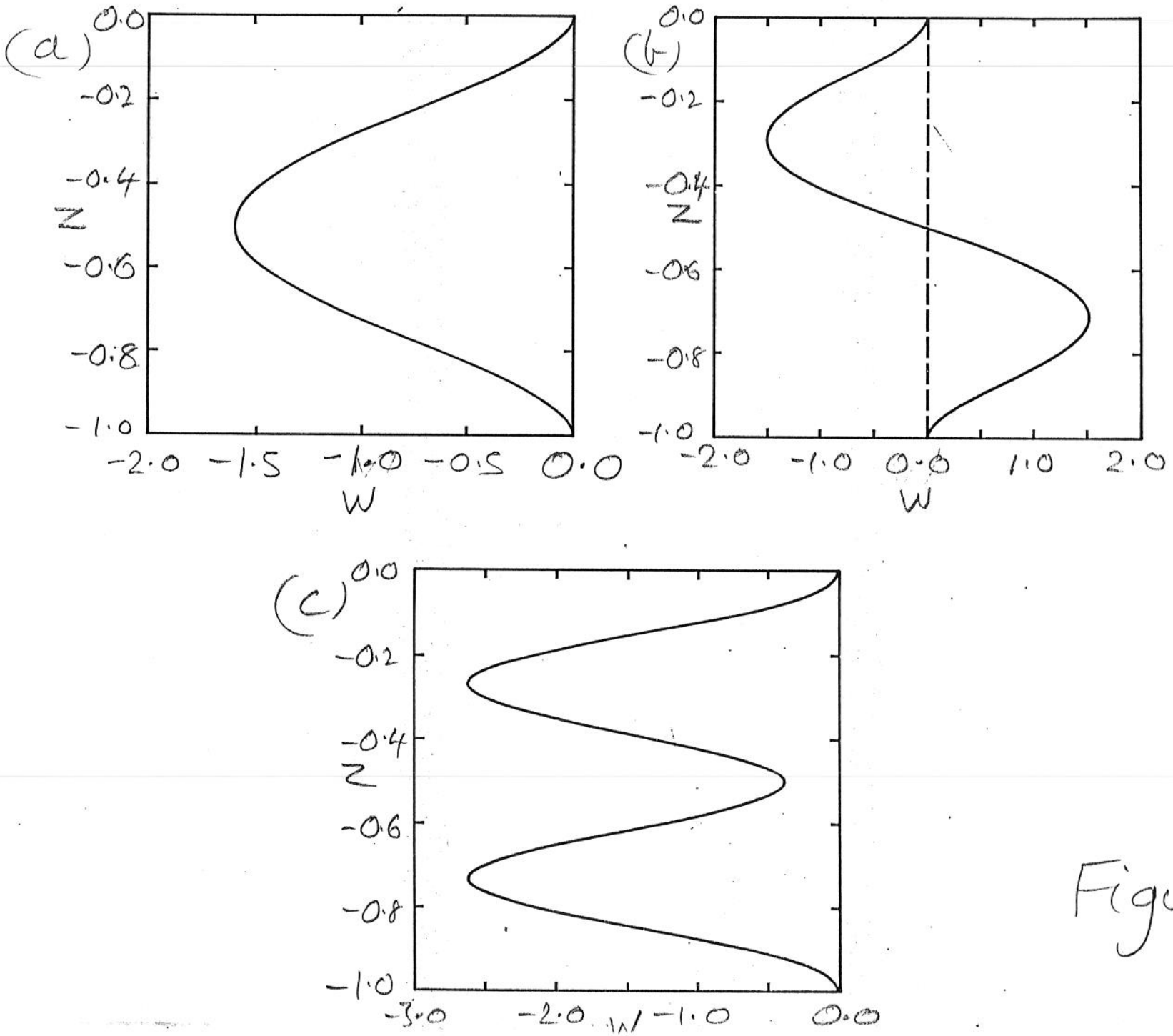
(a)
0.0
-0.2
-0.4
-0.6
-0.8
-1.0
z
-2.0
-1.5
-1.0
-0.5
0.0
w
(b)
0.0
-0.2
-0.4
-0.6
-0.8
-1.0
z
-2.0
-1.0
0.0
1.0
2.0
w
(c)
0.0
-0.2
-0.4
-0.6
-0.8
-1.0
z
-3.0
-2.0
-1.0
0.0
w

Figure 13